European Journal of Applied Sciences – Vol. 10, No. 2
Publication Date: April 25, 2022
DOI:10.14738/aivp.102.12077.
Simate, I. N., & Simukonda, K. (2022). Photovoltaic Forced Convection Greenhouse Solar Dryer with an Integrated Vertical Solar Collector for Mango Drying. European Journal of Applied Sciences, 10(2). 230-244.

Photovoltaic Forced Convection Greenhouse Solar Dryer with an Integrated Vertical Solar Collector for Mango Drying

Isaac N. Simate
Department of Agricultural Engineering, School of Engineering
University of Zambia, Lusaka, Zambia

Kondwani Simukonda
Department of Agricultural Engineering, School of Engineering
University of Zambia, Lusaka, Zambia

ABSTRACT

The design and experimentation of a Photovoltaic forced convection greenhouse solar dryer with a vertical solar collector incorporated inside the drying chamber for mango drying is presented. The integrated vertical solar collector combined the features of a south wall and a solar air heater to capture solar radiation that escapes through the south wall (north wall for the northern hemisphere) and heat the air before it enters the drying chamber. Mango drying experiments were carried out to ascertain the performance of the dryer. The solar radiation at the beginning of the experiments at 08:30 hours was 525.1 W/m^2, reaching a maximum of 1,133.0 W/m^2 shortly after midday and decreasing to 492.4 W/m^2 at 16:30 hours when the experiments were stopped. The ambient temperature and relative humidity ranged from 28.4 ^{0}C to 36.4 ^{0}C and 19.9% to 37.8%, respectively. Under these conditions, the air temperature inside the drying chamber was on average 14.7 ^{0}C above ambient, resulting in high drying rates such that the mango reached the moisture content of 13.7% wet basis after 7.5 hours of drying. The incorporation of a vertical solar collector inside the drying chamber helped, through storing heat in its mass, stabilise the drying chamber air temperature and made the forced convection dryer more compact thereby reducing usage of the space outside the dryer and making it available for other operations.

Keywords: Forced Convection, Greenhouse Solar Dryer, Mango Drying, Photovoltaic (PV), South Wall, Vertical Solar Collector

INTRODUCTION

Fruit and vegetable post-harvest losses are estimated to be as high as 50% of their production [1], and one way of reducing the losses is through solar drying. The advantages of solar drying over open sun drying are well established in many studies [2,3,4,5] having been carried out on different types of solar dryers. Among the advantages are that they have higher drying rates and produce better quality food compared to sun drying. For instance, Simate and Cherotich [6] carried out mango slices drying experiments in a natural convection solar tunnel dryer. The moisture content of the slices was reduced from 85.5% (wet basis) to 13.0% (wet basis) in 9.5 hours, thus showing the effectiveness of the method in preserving the mango. According to Simate [7] solar dryers can be broadly classified according to the method of heat transfer

(radiation, convection and conduction) to the drying material and the mode of airflow (natural, forced) through the dryer.

In the recent past, greenhouse structures have been converted into solar dryers operating in either natural or forced convection mode [8]. The conventional way of using the greenhouse as a solar dryer is to have an entry for fresh ambient air on one side of the greenhouse structure and an exit for warm humid air on the opposite side. This arrangement introduces cooler air into the greenhouse which lowers the inside temperature thereby slowing down the drying process.

Sahdev *et al*. [9] reviewed research on different types of greenhouse solar drying of various foods. The studies reviewed covered subjects such as dryer thermal analysis, drying characteristics of the foods, drying performance, energy and exergy analysis, and economic aspects. The major findings were that greenhouse solar drying took less time to dry foods, produced better quality foods and, had higher thermal efficiency than open sun drying. Gorjian *et al*. [10] reviewed the advancements in technical design and thermal performance enhancements of solar greenhouse dryers which include the integration with photovoltaic (PV) modules, use of the north wall to reduce heat loss from the dryer, use of thermal storage materials, and integration of solar air heaters for faster drying. The main findings of the review were that the advancements resulted in reduced drying time and better quality dried products. Sethi and Arora [11] incorporated an inclined north wall reflector to a conventional greenhouse solar dryer to increase the solar radiation available on the drying food. The reflector was used to capture radiation that was supposed to leave through the north wall of a conventional greenhouse solar dryer. The addition of the reflector increased the air and crop temperature which resulted in increased drying rate. Chauhan and Kumar [12] incorporated an insulated wall on the northern side of a greenhouse dryer to capture the incident solar radiation that escapes through the north wall. A further improvement on the dryer was the addition of a solar collector made of a black PVC sheet placed inside, on the floor of the dryer to eliminate the heat loss through the ground. The greenhouse dryer was operated under natural convection mode and its performance with the solar collector installed was found to be better than earlier developed greenhouse dryers. The highest temperature inside the greenhouse was 65.2 °C while the lowest relative humidity was 4.4% which are suitable for drying most fruits and vegetables. ELkhadraoui *et al.* [13] studied a solar greenhouse forced convection drying system essentially consisting of two parts, a flat plate solar air collector and a chapel-shaped greenhouse. The solar air collector was coupled to the greenhouse and supplied it with hot air. With this arrangement, the temperature inside the greenhouse dryer was found to be much higher than the ambient temperature while the relative humidity in the greenhouse was lower than that in the ambient. The result was that the drying time was reduced by one day and two days for red peppers and grape respectively. Román-Roldán *et al*. [14] carried out computational fluid dynamics analysis of heat transfer in a chapel-type greenhouse solar dryer coupled to an air solar heating system that heated the air before sending it to the greenhouse. The arrangement resulted in an almost homogeneous temperature distribution in the entire volume of the Greenhouse solar dryer making it suitable for good quality drying.

Among the thermal performance enhancements of solar greenhouse dryers, the use of an insulated north wall to reduce heat loss from the dryer and, the integration of solar air heaters

to supply hot air to the greenhouse solar dryer, are of particular importance to the current study as they form the basis for further improvements. The aim of this study was to combine the features of a north wall and a solar air heater into a vertical solar air collector integrated inside the greenhouse drying chamber. The addition of a solar collector inside the drying chamber would act as a thermal mass and help stabilise the air temperature inside the drying chamber. Since the greenhouse solar dryer would operate in the southern hemisphere, the vertical solar collector would capture radiation that escapes through the south wall (north wall for operation in the northern hemisphere) and heat the air before it enters the drying chamber.

MATERIALS AND METHODS

Description and Operation of the Greenhouse Dryer

The gable-even-span form of the greenhouse was selected for this study because it gives higher drying rates than other forms of greenhouses [15]. To improve the drying rate of the dryer in the current study, it was decided to preheat the ambient air with a solar air heater before the air enters the drying chamber. The dryer was therefore designed to have a vertical solar collector mounted inside the drying chamber to capture the solar radiation passing through the drying chamber and escaping through the south wall (for operation in the Southern Hemisphere). The collector absorber was made of a 0.3 mm-thick galvanized steel sheet painted matt black. Behind the absorber was a 50 mm airflow channel formed with the back plate followed by a 50 mm-thick glass wool insulation that has a thermal performance R value of 1.14 m^2K/W. In the airflow channel formed between the absorber and the back plate are 50 mm-wide vertical baffles arranged in such a way as to leave alternative spaces at the top and bottom of the channel for air to pass through in a zigzag manner. Previous work [16] on a solar collector with a baffled absorber that had a zigzag path for airflow, achieved thermal efficiency of 16 – 21% higher than the efficiency of a flat absorber with a smooth duct. The high efficiency was attributed to the higher heat transfer in the baffled absorber. The zigzag arrangement was therefore adopted in this study to ensure good heat transfer between the air and the absorber. Although a vertical inclination (90 degrees) for the collector was used in this study, it is recognized that this angle may not give the highest temperature as demonstrated by Mahdi and Gaddoa [17]. According to Twidell and Weir [18], for most applications, the best orientation for a fixed solar collector is facing the equator (due north in the southern hemisphere) with a slope equal to the latitude of the location. For this study, however, this orientation would take more horizontal space in the drying chamber and reduce the size of the food tray. Figure 1 shows the complete dryer with the collector installed inside the drying chamber.



Figure 1. Greenhouse Solar Dryer

The entrance of air into the collector is through an opening that protrudes through the front glazing to the outside of the drying chamber. At the opposite end of the inlet to the collector is the outlet for heated air from the collector. A 12 V DC fan (Sunon Megalev 12 V DC, 10 W, 3.86 m^3/min) mounted to the collector outlet pulls air heated by the collector and blows it over the food tray. Figure 2 is a view of the inside of the drying chamber showing the collector with the fan fixed to the collector outlet and a rail at the bottom of the collector for supporting the food tray.



Figure 2. View inside the drying chamber

The air which has been used in the drying chamber is expelled from the dryer using a smaller 12 V DC fan (Sunnon 12 V DC, 1.7 W, 1.15 m^3/min) positioned at the apex of the drying chamber as shown in Figures 1 and 3. Both fans are powered by a 10 W solar PV panel connected directly to the fans. Initial trials with bigger capacity fans to expel air from the dryer, resulted in lower

temperatures in the drying chamber as a result of higher airflow which would lower the drying rate.



Figure 3. Solar dryer front view showing the drying chamber exit fan at the apex of the greenhouse

To come up with the size of the dryer, previous criteria used in the design of solar tunnel dryers [19; 20] was adopted and this requires the collector to have the same area as the drying section. The area for the drying section requires knowledge of the loading density. Previous works on mango drying [6; 21] have reported a loading density for mango as 2.6 kg/m^2. Therefore, starting with a mass (in kg) of mango to be dried, the area of the food tray was determined which was also the area for the collector. A mass of 1.3 kg was considered which gave a drying area of 0.5 m^2 and this was taken to be the same as the collector area. The final dimensions of the dryer were calculated as length 1.09 m, width 0.65 m, height of the long sides 0.6 m, and height of the apex 0.81 m giving a volume of 0.5 m^3 for the drying chamber. The floor of the drying chamber was insulated with the same glass wool as used for the collector back. The roof and the three sides, except the south wall, were covered with a 1 mm-thick clear polycarbonate sheet to allow entry of solar radiation into the dryer.

The dryer operated as a forced convection mixed-mode solar dryer where the drying food received both direct solar radiation and hot air from the collector circulated by the PV-driven fans.

Experimental Procedure

Initial moisture content of mango

Fresh, ripe but firm mangoes were obtained locally from the market for the experiments. To determine the initial moisture content, the standard method of moisture content determination [22] was used. The mangoes were washed using clean tap water then peeled and cut into 3-mm thick slices using a table knife. About 10 g of the sliced mango was put into each of the three aluminium dishes, the weight having been checked with a digital balance (Mettler Instruments BV, Switzerland, model PE 3000, maximum weighing capacity: 3,100g, sensitivity: 0.1g,

accuracy, ±0.1 g). The three dishes loaded with samples were then put into the oven set at a temperature of 105 °C for 3 hours. At the end of the three hours, the samples were weighed again. The moisture content (wet basis) was then calculated as the ratio of weight lost by the sample to the initial weight of the sample.

Greenhouse Solar Drying Experiment

The solar drying experiment was carried out at the Department of Agricultural Engineering of the University of Zambia, Lusaka, located at latitude 15.3 ^{0}S and longitude 28.3 ^{0}E during the month of December. Mangoes from the same batch as the ones used for the initial moisture content determination were used in the drying experiment. Three sample trays made of plastic mesh (size 0.1 m by 0.1 m) were each loaded with 20 g of the 3-mm mango slices for the purpose of weight loss measurements. The sample trays containing the mango slices were then loaded onto a bigger drying tray (size 0.95 m by 0.52 m) located in the drying unit. The first sample tray was positioned closest to the collector exit fan, the second tray in the centre of the big tray and, the third tray was the furthest from the fan, i.e. at the opposite end of the big tray. The rest of the drying tray area was then covered with the mango slices, ensuring that the slices did not touch each other. The total mass of the mango slices loaded in the dryer was 1.3 kg.

Temperature probes (Campbell Scientific Inc., model: 108– L accuracy ±0.01 ^{0}C) with a measuring temperature range of −5 to +95 ^{0}C were used to measure air temperatures at the collector exit, drying chamber exit and in the ambient. Relative humidity in the ambient was measured with a relative humidity probe (Campbell Scientific Inc., model: HMP35D; accuracy at +20 ^{0}C is ±2% RH (0–90% RH) and ±3% RH (90–100% RH)). A Solarimeter (Kipp & Zonen Delft BV, model: CM11, irradiance range: 0 – 1,400W/m^2, sensitivity: between 4 and 6μV/Wm^{-2}) placed near the solar dryer was used to measure solar radiation. All the probes were connected to a multiprobe data logger (Campbell Scientific Inc., model: CR 1000) which recorded the air temperatures, relative humidity, and solar radiation. The airflow at the exit of the drying chamber was measured with a digital anemometer (Toptronic, T8000 measurement range: 0.4 to 30.0 m/s). Figure 4 shows the instruments and solar panel used in the drying experiment.



(a) (b)



(c) (d)

Figure 4. Instrumentation and solar panel used in the experiment; (a) Electronic Balance, (b) Solarimeter, (c) Airflow Meter, Laptop and Data Logger and (d) Solar Panel

The drying experiment started at 08:30 hours and ended at 16:30 hours giving an eight-hour drying period. The weight loss of the mango slices was monitored by weighing the three sample trays using the digital balance, while the airflow was measured by placing the digital anemometer at the drying chamber exit in front of the small fan, and both measurements were done every 30 minutes. The solar radiation, temperature and relative humidity in the dryer and ambient were recorded by the data logger.

Uncertainties and Errors in the measurements

In carrying out this experiment, it was recognised that errors and uncertainties could have occurred that relate to the setup of the experiment, instrument calibration and resolution, and inaccuracy in reading the instruments. The overall uncertainty is given in equation 1 by NASA [23].

$$U_{over} = \left(U_{bia}^2 + U_{ran}^2 + U_{res}^2 + U_{ope}^2 + U_{env}^2\right)^{0.5} \quad (1)$$

Where: U_{over} is the overall uncertainty; U_{bia} is the uncertainty as a result of reference attribute bias that persists during a measurement session; U_{ran} is the uncertainty due to repeat measurement which shows itself as differences in the measured value from one measurement to another during a measurement session; U_{res} is the uncertainty due to the smallest discernible value shown in a measurement; U_{ope} is the uncertainty due to errors introduced when the person taking the measurement produces a systematic bias towards a measurement; and U_{env} is the uncertainty due to errors introduced by changing environmental conditions such as solar radiation, temperature and humidity.

The Overall Uncertainty U_{over} for each of the measured parameters (Solar Radiation, Air Temperature, Relative Humidity, Sample Weight, Airflow) was calculated using equation 1.

RESULTS AND DISCUSSION

Uncertainty Analyses

Table 1 shows the uncertainties in the parameters measured as calculated using methods described by NASA [23]. The temperature measurement was the only contributor to the overall uncertainty of bias (U_{bia}) measurement which was considered to be normally distributed with a containment probability of 97.5%. The random uncertainty (U_{ran}) was not considered for all the measured parameters since their values changed throughout the experiment due to changes in solar radiation. For the uncertainty due to resolutions of measuring instruments (U_{res}), only the measurement of sample weight and airflow were considered since the operator read and recorded these measurements; and the error was considered to be uniformly distributed with 100% containment probability. The operator uncertainty error (U_{ope}) was not considered for solar radiation, air temperature and relative humidity measurements as these were recorded automatically by the data logger and only handled during the setup of the experiment. However, for the measurement of sample weight and airflow which were done every 30 minutes, operator influence was considered present and the uncertainty error was considered to be normally distributed. The containment probability was taken as 90% while the limits were assumed to be half of the resolution error. The environmental uncertainty (U_{env}) could have been affected by solar radiation, ambient temperature and wind. The measurement probes were not under direct solar radiation while changes in air temperature were related to the ambient temperature. The balance for measuring sample weight was put in the place shielded from direct solar radiation and wind. However, the measurement of airflow, which was done at the drying chamber exit could have been affected by wind, and the uncertainty was assumed to be ±0.05 m/s.

Table 1. Uncertainties in measured parameters

Parameter	U_{bia}	U_{ran}	U_{res}	U_{ope}	U_{env}	U_{over}
Solar Radiation, W/m^2	±4.46	0	0	0	±2	±4.89
Air Temperature, ^{0}C	±0.134	0	0	0	0	±0.134
Relative Humidity, %	±0.89	0	0	0	±0.04	±0.89
Sample Weight, kg	±0.04	0	±0.06	±0.03	0	±0.08
Air flow, m/s	±0.04	0	±0.06	±0.03	±0.05	±0.09

Drying Experiments

The determination of the initial moisture content of mango gave an average value of 88.2% on wet basis. Previous studies on mango found moisture contents of 85.5% [6] and 84% [24].

The ambient conditions which influenced the drying process were solar radiation, air temperature and relative humidity. The variation of solar radiation with drying time, as the day progressed, is shown in Figure 5. The graph follows a typical trend of solar radiation, starting with a low value of 525.1 W/m^2 in the morning at 08:30 hours, reaching a maximum of 1,133.0 W/m^2 shortly after midday and decreasing towards the late afternoon to a value of 492.4 W/m^2 at 16:30 hours when the experiment was stopped. The fluctuations in the graph are due to intermittent cloud cover.

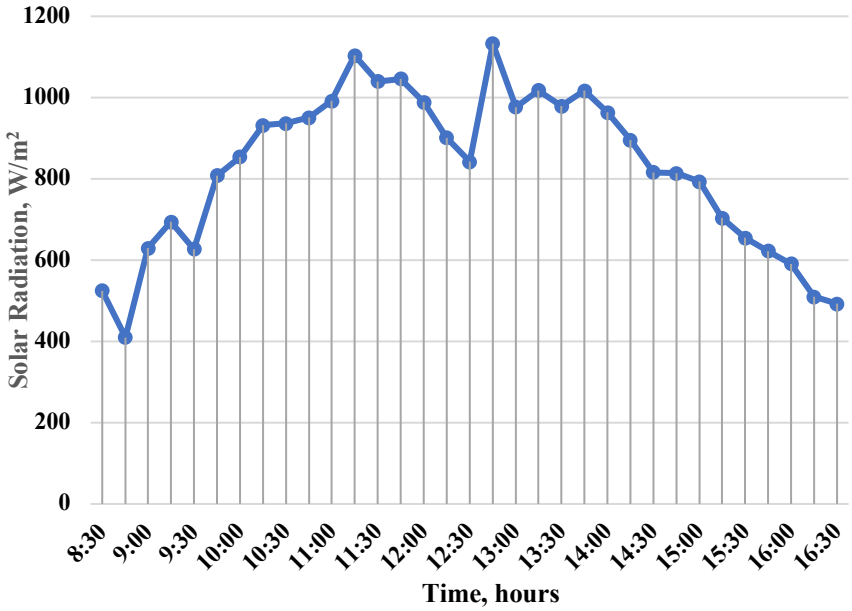

Figure 5. Solar radiation changes with time of the day

Figure 6 shows the temperature and relative humidity in the ambient. The general trend is that as the temperature increases, the relative humidity decreases making the air increase its moisture carrying capacity. When this air enters the collector, it is heated further and its relative humidity is reduced further, making it have a bigger capacity to carry moisture from the drying mango slices in the drying chamber.

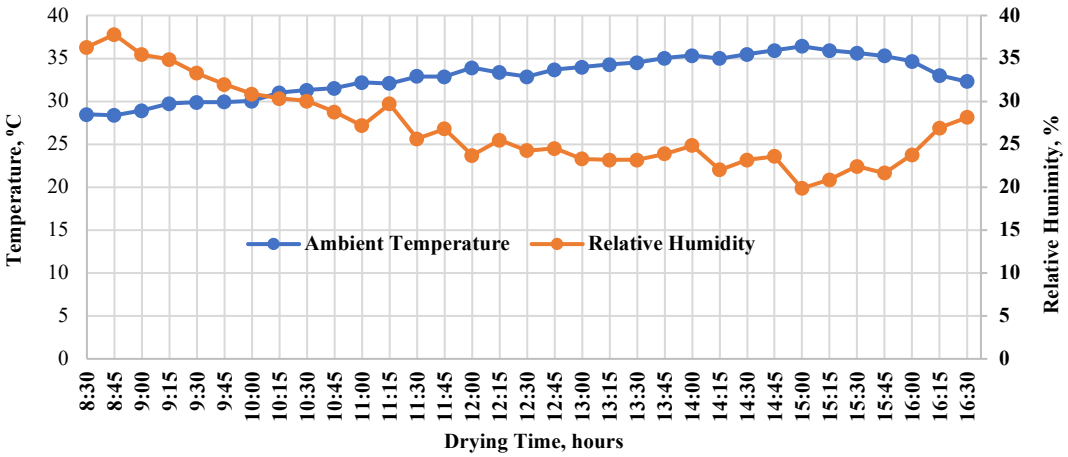

Figure 6. Temperature and Relative Humidity in the ambient

Figure 7 shows the air temperatures at the collector exit and in the drying chamber. The influence of collector exit air temperature on the drying chamber air temperature is quite evident from the patterns of the two curves as they are similar and almost equal, differing by an average of 1.1 ^{0}C. As a result of this arrangement, the drying chamber temperature is higher than the ambient temperature by an average of 14.7 ^{0}C. The collector captured the solar radiation that would have escaped through the south wall of the greenhouse drying chamber.

The main advantage of having a collector inside the drying chamber is that the air entering the drying chamber is already heated to a temperature above ambient and therefore helps maintain high temperatures in the drying chamber as opposed to cooler air entering the drying chamber from the ambient as the case is with conventional greenhouse solar dryers. It is further noted that due to its mass, the collector behaved as a thermal mass and helped stabilize the drying chamber temperature. With this new arrangement, it is possible to achieve higher drying rates which translate into shorter drying times. A similar result was obtained by Román-Roldán *et al.* [10] who carried out computational fluid dynamics analysis of heat transfer in a chapel-type greenhouse solar dryer coupled to an external solar air heating system which heated the air before sending it to the greenhouse. The average temperature of the air inside the greenhouse was 14 ^{0}C above the ambient temperature and therefore suitable for drying.

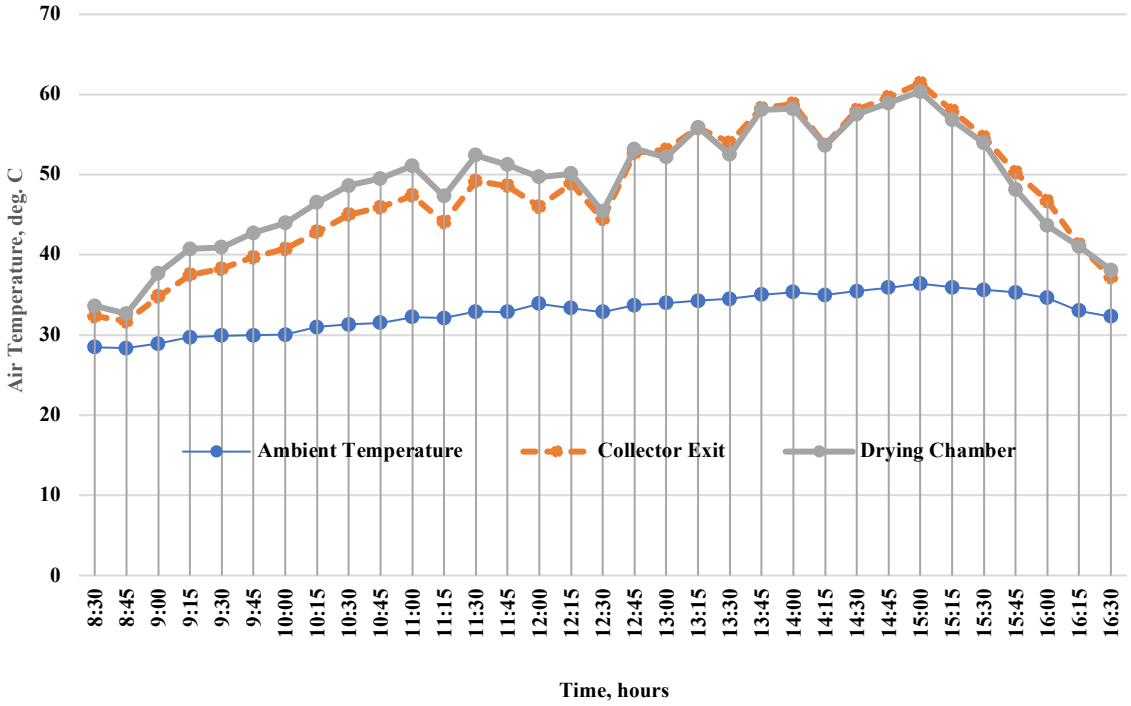

Figure 7. Air temperature at Collector Exit and in the Drying Chamber

The variation of airflow with time is shown in Figure 8. The measurements of airflow were done at 30 minutes intervals and therefore give values of airflow at particular points in time during the drying experiment.The airflow fluctuated with a minimum of 0.0186 kg/s and a maximum of 0.0409 kg/s, and follows a similar trend to that of solar radiation shown in Figure 5. The fluctuations in the airflow are a direct response to the intermitted cloud cover which directly affected the power output from the solar panel that supplied the power to the fans. The average airflow was determined as 0.032 kg/s which is comparable to the range of 0.014 to 0.036 kg/s used by Akbulut and Durmus [25] in studying energy and exergy of forced convection solar drying of mulberry. Their results showed reduced drying time at higher airflow. Bala and Woods [26] reported that the airflow during the drying process has two functions. The first function is of supplying heat to evaporate moisture from the food and the other is of taking away the evaporated moisture to the outside of the dryer. Simate [27] considered airflow as

one of the main factors that affect the performance of solar dryers and that understanding its behaviour could help design better performance solar dryers.

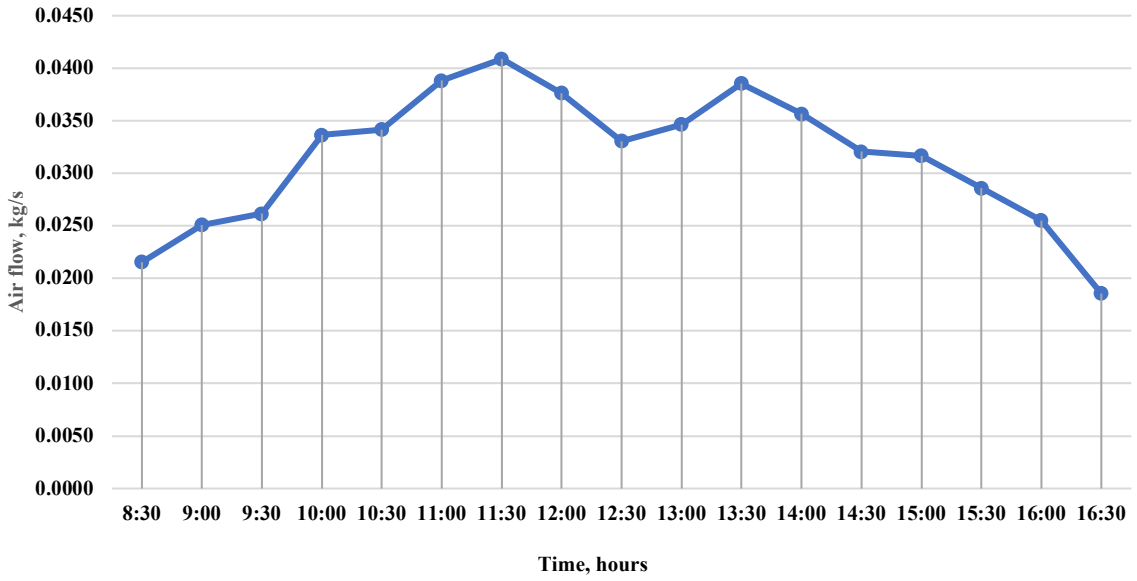

Figure 8. Variation of Airflow with time

The moisture curves of the three samples in the big drying tray are shown in Figure 9 which indicates the effect of the airflow from the fan on the moisture reduction in the samples. Sample MC1 was the closest to the collector exit fan. It received the hottest air from the collector and the highest airflow, followed by sample MC2 which was placed in the centre of the tray and lastly, sample MC3 was the furthest from the fan at the opposite end of the tray. Sample MC1 reached the 15 % moisture content earlier than the other two samples and this can be attributed to the sample receiving the highest temperature and airflow. On average, the samples reached a moisture content of 13.7% w.b. after 7.5 hours of drying which is below the safe moisture content of 15% recommended for storage. According to Nyangena *et al*. [28] dried mango slices can be preserved for longer periods if they have a moisture content of 15% or less. This level of moisture content inhibits the growth of micro-organisms.

Kanokwan *et al*. [29] dried mango slices of 2 mm thickness in a greenhouse solar dryer that was covered with a double layer of polycarbonate and mounted on a concrete floor. The maximum solar radiation recorded was 955 W/m^2 which resulted in a temperature range of 26.7 ^{0}C to 59.1 ^{0}C inside the dryer. Under these conditions, the mango slices were dried from an initial moisture content of 85.6% w.b. to 12.5% w.b. in 7 hours. These results can be compared to the current study where bigger mango slices of 3 mm thickness were dried from 88.2% w.b. to 13.7% w.b. in 7.5 hours of drying under drying chamber temperature of 32.6 ^{0}C to 60.4 ^{0}C where the maximum solar radiation recorded was 1,133 W/m^2. The result in the current study shows that this new design is very effective in reducing the moisture content of mango slices.

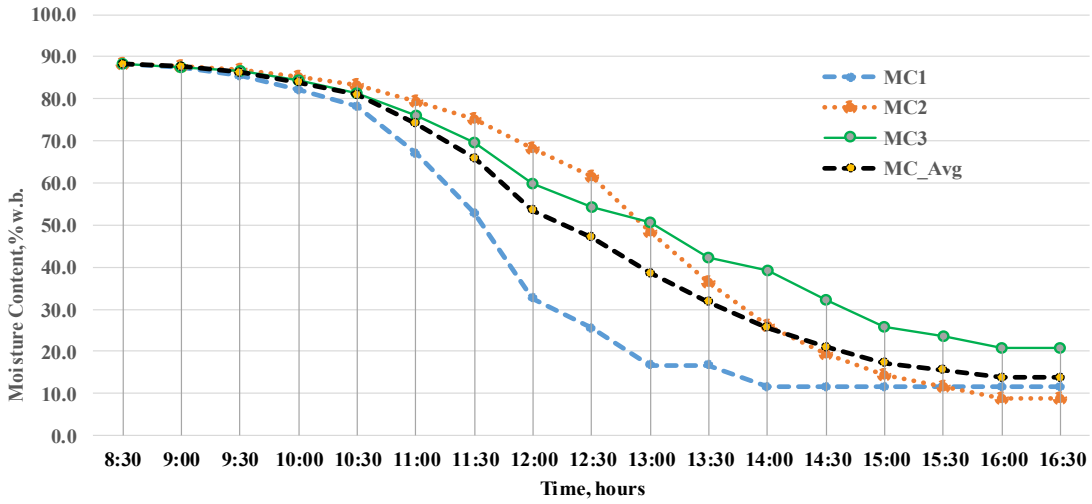

Figure 9. Moisture curves (MC1 = moisture content of sample nearest the fan at collector exit, MC2 = moisture content of sample in the centre of the tray, MC3 = moisture content of sample furthest from the collector exit fan and, MC_Avg = the average moisture content

Figure 10 shows the drying rate with respect to time. These drying rate curves were obtained by differentiating the moisture curves in Figure 9 and are characterised by oscillations. Kemp *et al.* [30] reported that the drying rate curves, obtained by differentiation of the moisture curves, usually have significant amounts of noise even though the moisture content curves may be smooth. The general behaviour of the three curves is that the drying rate increases rapidly in the first one hour of drying and then oscillates around a value of 2.0 kg/h from 09:30 hours to 10:30 hours. Then, from 10:30 hours to 14:00 hours, there is a continuous reduction, and lastly from 14:00 hours to 16:00 hours, it remains constant. The period from 09:30 hours to 10:30 hours, where the drying rate oscillates about a constant drying rate of 2.0 kg/h, can be related to the heat transfer controlled phase, whereas the period from 10.30 hours to 14:00 hours, where the drying rate is falling continuously, is limited by internal moisture transport. The 10.30 hours point where the constant rate and falling rate meet and change from one rate to the other, i.e. the critical point, is not evident from the graphs. According to Kemp et al. [26], a sharp transition from constant rate to falling rate drying period is very rare, and usually, the critical moisture content is determined by projecting fitted lines of the constant and falling rate periods. Earle [30] pointed out that many foods do not show a true constant rate drying period.

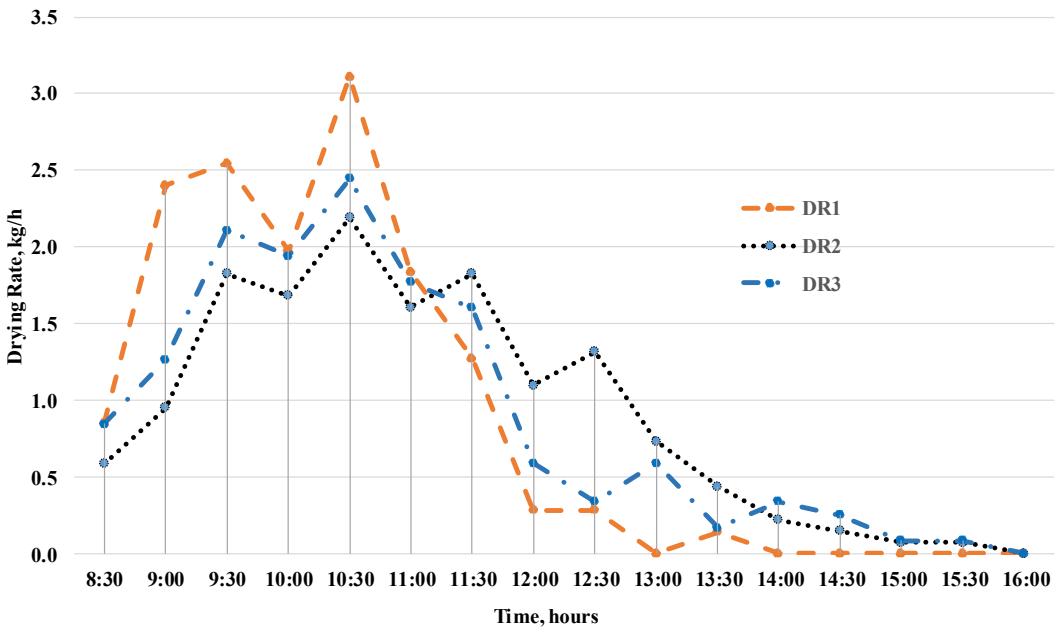

Figure 10. Drying Rates ((DR1 = Drying Rate of sample nearest the fan at collector exit, DR2 = Drying Rate of sample in the centre of the tray, DR3 = Drying Rate of sample furthest from the collector exit fan

CONCLUSION

A greenhouse solar dryer with a vertical solar collector, integrated within the drying chamber and heating air from ambient before being used in the drying chamber, was developed and tested on drying mango slices.

The airflow in the solar collector and drying chamber, driven by 12 V DC fans that were directly powered by a solar PV panel, fluctuated in response to the intermitted cloud cover. The magnitude of fluctuations in the airflow did not seem to be the same as those in the collector and drying chamber temperatures, which also fluctuated. This could be attributed to the collector behaving as a thermal mass and being slow in responding to solar radiation changes compared to the fans supplying air. For the airflow, the resulting average of 0.032 kg/s was comparable to similar studies and helped reduce the drying time as was evident in the sample closest to the collector exit fan that reached the safe moisture content earlier than the other samples.

Mounting the solar collector inside the drying chamber was found beneficial because it:

- Captured the solar radiation that would normally enter the drying chamber but escape through the South wall (for operation in the Southern Hemisphere) in a conventional greenhouse dryer.
- Helped, through storing heat in its mass and pre-heating incoming ambient air, maintain high temperatures in the drying chamber which were on average 14.7 ^{0}C above ambient resulting in the mango reaching the moisture content of 13.7% wet basis, which is below the safe moisture content of 15%, after 7.5 hours of drying.
- Made the dryer more compact and reduced space usage outside the dryer. The saved space could be used for other operations.

Further studies on this dryer could include optimization to look at the cost-drying rate relationship, which is important in scaling up the size of the solar dryer.

References

Phiri, A., *Post-harvest Losses of Fruits and Vegetables in Zambia*. AARDO Workshop on Technology on Reducing Post-harvest Losses and Maintaining Quality of Fruits and Vegetables, 2010: p. 197–204. http://ir.tari.gov.tw:8080/bitstream/345210000/2830/1/publication no147 21.pdf.

Daud, L.E., and I.N. Simate, *Drying Kinetics of Sliced Pineapples in a Solar Conduction Dryer*. Energy and Environment Research, 2017. 7(2): https://doi.org/10.5539/eer.v7n2p14

Molefe, M.J., and I.N. Simate, *Thin Layer Drying and Modelling of Poultry Litter Briquettes*. Energy and Environment Research, 2019. 9(1): https://doi.org/10.5539/eer.v9n1p9

Janjai, S. *A greenhouse type solar dryer for small-scale dried food industries: Development and dissemination.* International Journal of Energy and Environment, 2012. 3 (3): p 383-398.

Ssemwanga, M. et al., *The effect of traditional and improved solar drying methods on the sensory quality and nutritional composition of fruits: A case of mangoes and pineapples*. Heliyon, 2020. 6: https://doi.org/10.1016/j.heliyon.2020.e04163.

Simate, I.N., and S. Cherotich, *Design and Testing of a Natural Convection Solar Tunnel Dryer for Mango*. Hindawi Journal of Solar Energy, 2017. Article ID 4525141. https://doi.org/10.1155/2017/4525141

Simate, I.N., *Energy and Exergy Analysis of an Indirect-Mode Natural Convection Solar Dryer for Maize*. Energy and Environment Research, 2021.11(2):p. 19-30. https://doi.org/10.5539/eer.v11n2p19

Prakash, O., et al., *Performance of modified greenhouse dryer with thermal energy storage*. Energy Reports 2, 2016: p. 155–162. http://dx.doi.org/10.1016/j.rser.2013.08.084

Sahdev, R.K., et al., *A review on applications of greenhouse drying and its performance*. Agric.Eng.Int: CIGR Journal Open access, 2016. 18, (2):p. 395 – 412. http://www.cigrjournal.org.

Gorjian, S., et al., *Recent Advancements in Technical Design and Thermal Performance Enhancement of Solar Greenhouse Dryers*. Sustainability, 2021.13, 7025. https://doi.org/10.3390/su13137025

Sethi V.P., and S. Arora, *Improvement in greenhouse solar drying using inclined north wall reflection.* Solar Energy, 2009. 83: p. 1472–1484. DOI:10.1016/j.solener.2009.04.001

Chauhan, P. S., and A. Kumar, *Performance analysis of greenhouse dryer by using insulated north-wall under natural convection mode*. Energy Reports, 2016.2: p.107-116. http://dx.doi.org/10.1016/j.egyr.2016.05.004

ELkhadraoui, A., et al., *Experimental investigation and economic evaluation of a new mixed mode solar greenhouse dryer for drying of red pepper and grape*. Renewable Energy, 2015.77:p.1–8. https://doi.org/10.1016/j.renene.2014.11.090

Román-Roldán, N-I., et al., *Computational fluid dynamics analysis of heat transfer in a greenhouse solar dryer "chapel-type" coupled to an air solar heating system*. Energy Science and Engineering, 2019. 7:p.1123 - 1139. https://doi.org/10.1002/ese3.333

Kassem, A.M., *Effect of architectural form of greenhouse solar dryer system on drying of onion flakes*. Egypt J. Agric. Res., 2011. 89 (2): p. 627-638. https://ejar.journals.ekb.eg/article_175949.html

Singh, V., et al., *Experimental Investigation of Double Pass Solar Air Heater with Baffled Absorber Plate*. International Journal of Scientific Research in Science, Engineering and Technology, 2017. 3(8):p.163-170.

Mahdi, M.M., and A.A. Gaddoa, O*utdoor Testing of a Zig-Zag Solar Air heater with and without Artificial Roughness on Absorber Plate*. Journal of Engineering, 2019. 4(25): https://doi.org/ 10.31026/j.eng.2019.04.01

Twidell, J. and T. Weir, *Renewable Energy Resources*, Second Edition, 2006.Taylor and Francis, ISBN 0–419–25330–0.

Schirmer, P., et al., *Experimental investigation of the performance of the solar tunnel dryer for drying bananas*. Journal of Renewable Energy, 1996.7(2): p. 119–129.

Bala, B.K., et al., *Solar drying of pineapple using solar tunnel drier*. Journal of Renewable Energy, 2003. 28 (2): p. 183-190. https://doi.org/10.1016/S0960-1481(02)00034-4

Cherotich, S., and I. N. Simate, *Experimental investigation and mathematical modelling of a natural convection solar tunnel dryer.* International Journal of Scientific & Engineering Research, 2016.7 (5): p. 597-603. ISSN 2229-5518

AOAC, *Determination of Moisture, Ash, Protein and Fat*, *Official methods of analysis*. Association of Official Analytical Chemists International, 2005. Washington DC.

National Aeronautics and Space Administration, *Measurement Uncertainty Analysis Principles and Methods*. NASA Measurement Quality Assurance Handbook—ANNEX 3, NASA-HDBK- 8739.19-3, 2010. National Aeronautics and Space Administration, Washington D.C.,WA, USA.

Touré, S. and S. Kibangu-Nkembo, *Comparable study of natural solar drying of cassava, banana and mango*. Journal of Renewable Energy, 2004. 29(6): p.975-990. http://dx.doi.org/10.1016/j.renene.2003.09.013

Akbulut, A., and A. Durmus, *Energy and exergy analyses of thin layer drying of mulberry in a forced solar dryer*, Energy, 2010. 35 (4):p 1754-1763. https://doi.org/10.1016/j.energy.2009.12.028

Bala, B. K., and J. L. Woods, *Simulation of the Indirect Natural Convection Solar Drying of Rough Rice*. Solar Energy, 1994. 53(3): p 259-266. https://doi.org/10.1016/0038-092X(94)90632-7

Simate, I.N., *Air Flow Model for Mixed-mode and Indirect-mode Natural Convection Solar Drying of Maize*. Energy and Environment Research, 2020. 10 (2): ISSN 1927-0569 E-ISSN 1927-0577. https://doi.org/10.5539/eer.v10n2p1.

Nyangena, I., et al., *Moisture sorption properties of two varieties of dehydrated mango slices as determined by gravimetric method using Guggenheim-Anderson-de Boer model*. Journal of Food Processing and Preservation, 2020. https://doi.org/10.1111/jfpp.15041

Kanokwan, K., et al. *Comparison of Performance and Economic Efficiency for Greenhouse Solar versus Hot Air Drying: A Case of Crispy Mango Production*. Processes, 2022. 10, 311. https://doi.org/10.3390/pr10020311

Kemp, I.C., et al., *Methods for Processing Experimental Drying Kinetics Data.* Drying Technology: An International Journal, 2001. 19(1): p 15-34. http://dx.doi.org/10.1081/DRT-100001350

Earle, R. L., *Unit Operations in Food Processing*. 2nd edition 1983, Oxford: Pergamon Press (United Kingdom).